Singla et al. 2018. *Int. J. Vehicle Structures & Systems*, 10(3), 184-187
ISSN: 0975-3060 (Print), 0975-3540 (Online)
doi: 10.4273/ijvss.10.3.06

International Journal of Vehicle Structures & Systems
Available online at www.maftree.org/eja

Microstructural and Mechanical Investigations of Mg-based Alloys

Amit Singla[a,b,c], Neeraj Sharma[a] and Sushil Kumar[a]

[a]*Dept. of Mech. Engg., Maharaja Agrasen University, Baddi, Himachal Pradesh, India*
[b]*Mech. Engg. Dept., Maharishi Markandeshwar (Deemed to be University), Mullana, Haryana, India*
[c]*Corresponding Author, Email: amit.singla97@gmail.com*

ABSTRACT:

In the present work, an attempt has been made to study the microstructural and mechanical behaviour of Mg-alloy prepared by powder metallurgy process. Highly pure Mg powder is used for the fabrication of Mg-alloy at different additive percentages. The investigation of constituent phases was successfully completed for the Mg-alloy using standard X-ray diffractometers. Scanning electron microscopy was used for the morphological studies. Tensile strength and percentage elongation of Mg-alloys were also evaluated at room temperature. The minimum and maximum ultimate stress varies from 67 to 108MPa. The percentage elongation also increased 1.03 to 1.57%.

KEYWORDS:

Microstructure; Powder metallurgy; Magnesium alloy; Tensile strength

CITATION:

A. Singla, N. Sharma and S. Kumar. 2018. Microstructural and Mechanical Investigations of Mg-based Alloys, *Int. J. Vehicle Structures & Systems*, 10(3), 184-187. doi: 10.4273/ijvss.10.3.06.

1. Introduction

Magnesium is the sixth most abundant element on earth's crust and due to its high stiffness, non-flammability and lightweight it has been approved for structural applications, including its use inside aircraft cabin. The automotive companies are also in a pursuit to replace it with dense materials of automobiles to decrease the structural weight and improve the fuel economy [1]. Due to hexagonal closed pack crystal structure of Mg, it shows poor formability and secondary processing induced crystallographic asymmetry [2]. This is one the main limitations of Mg alloys. Different researchers worked on the alloying elements of Mg to enhance its mechanical properties, corrosion rate, biocompatibility and biodegradability [3-6]. Out of all these the rare earth (RE) metals gives promising results. Every individual rare earth metal has its own characteristic and chemistry with Mg [7]. Tekumalla et al. [8] presented a detailed review work on the mechanical characteristics of Mg and RE combination in binary, ternary and higher alloy. A small amount of RE in Mg can significantly affect the characteristics of Mg-RE alloy. The non-toxic and biocompatible nature of Mg makes it suitable for medical applications [9-10].

Other biomedical alloys are metals (cobalt-chrome steel, stainless steel, Ti, alloys), ceramic (bio-active glass, calcium phosphate, Alumina Al_2O_3, Zirconia ZrO_2) and polymers (silicon rubber, acrylic resin). These biomaterials are categorized in three different generations like first generation biomaterial, second generation and third generation biomaterial. The synthetic materials which were selected depending upon their physical properties (nearby the replaced tissue) and minimal toxic response are known as first generation biomaterial. The toxicity and mechanical properties plays a significant role in the selection of implant material. This would elicit fibrous capsule around the material which helps to isolate it from surrounding tissue. The bioactive materials which have the ability to interact with the biological environment to increase its biological response and tissue bonding are known as second generation bio-materials. These biomaterials degrade while new tissue regenerate and heals. The second generation biomaterials include bioactive glass, biodegradable polymer of synthetic and natural origin. The third generation biomaterials are the bio-resorbable and bioactive materials which have porous 3D structure and are able to stimulate regeneration of living tissue and activate genes [11-12]. The biomedical implant market is expected to garner $116bn by 2022 and this is increasing at a rate of seven percent per year.

The development of biodegradable material can reduce the expense of remove, refit and re-implant [13]. There are three types of biodegradable materials i.e. Fe-based, Mg-based and Zn-based. The biodegradability depended upon the corrosion rate of the material in bio-fluid. Initially material provides its required function of support and tissue generation, after that it degradation starts. The tissue healing rate and degradation rate of alloy should be matched for a good biodegradable implant [14-17]. Some of the material is consumed by the body according to the requirement of daily consumption. Daily consumption of materials by human body plays a major role in the biomaterial selection [18]. The corrosion rate of Fe-based alloys is low, Mg-based alloys is high and Zn-based alloys is in between the Fe-based and Mg-based [16]. Mg-based alloy acts as a research vanguard as compared to other materials, which makes it a potential candidate for automotive application. Due to its form type structure it can absorb

the vibrations. Also the applications of Mg-alloys are found in implants. So, its microstructural investigations can open numerous lines of research. Some future directions of present research were also discussed in the conclusion section.

2. Material and method

2.1. Material preparation

Commercially available pure Mg (99.95%) powder is used for the fabrication of Mg form by powder metallurgy process. The mixing or blending time has a significant role in homogeneity and crystal size reduction of metal powders [19]. Initially this powder was compacted in a die with 2% of additive (1% binder and 1% water) after that two more samples were also generated at 4% (2% binder and 2% water) and 6% (3% binder and 3% water additive). The green compact is brittle in nature, so sintering is carried out at 0.6-0.7 times of melting temperature of Mg. In the present work, sintering is processed at 410°C. Due to the reactive nature of Mg, argon gas (highly pure up to 99.999%) is supplied during sintering process to avoid any chance of oxidation/reduction. Each sample was mechanically polished up to 2000 grit, ultrasonically cleaned in acetone, absolute ethanol and distilled water, and then dried in open air.

2.2. Microstructural characterization

Jeol make scanning electron microscopy is used for the observation of morphology of Mg-form. Specimens were imaged at 20 kV by scanning electron microscope. PANalytical X'pert PRO X-ray diffractometer was used for recording the X-ray diffraction (XRD) patterns with CuK radiation (λ=1.54A˚). XRD was completed for the investigation of the constituent phases in Mg-alloy.

2.3. Mechanical characterization

Tensile tests were performed on cylindrical samples using computerized Universal Testing Machine (UTM) to find out the Yield Strength (YS) and Ultimate Strength (US). Elongation in the specimen was measured with the help of extensometer attached with the UTM. Load cell resolution for the UTM was 100N and experiment was performed at a constant rate of 0.05mm/min.

3. Results and discussions

3.1. Microstructural behaviour

Fig. 1 shows sample of open-cell Mg-foams with varying pore sizes in the order of 0.42mm. From this image, it can be evident that the porosity has been homogeneously distributed in the specimen. The space holders (organic particles) were evaporated from the Mg-alloys and made the space for pore size and shape. Fig. clearly reveals the interconnectivity of alloy open porosity. The Mg-form is characterized by XRD for their phase composition, and the results show that it is composed of one single phase of Mg as shown in Fig. 2. The different orientations of Mg are observed at different angle. Refinement in the crystalline size was assumed the main reason for broaden the peaks. To find out the crystallite size of compound Williamson-Hall formula [20] as below was used:

$$\sqrt{\left(B_i^2 - B_o^2\right)}Cos\theta = 0.89\frac{\lambda}{d} + 2eSin\theta \quad (1)$$

Where B_i – XRD pattern's peak full width when maximum intensity is half, B_o - Instrument broadening correction factor, θ - Bragg angle, e - Lattice strain, λ - wave-length of X-ray, d - Crystallite size.

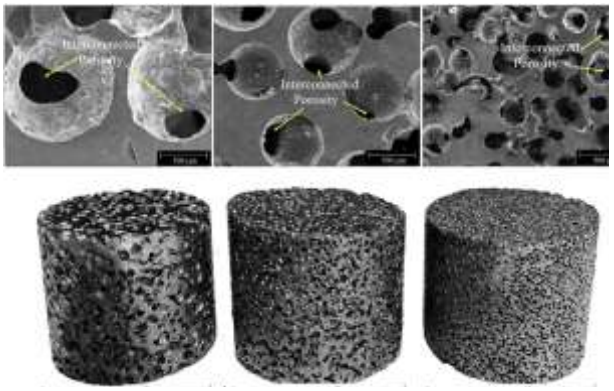

Fig. 1: Open-cell Mg foam

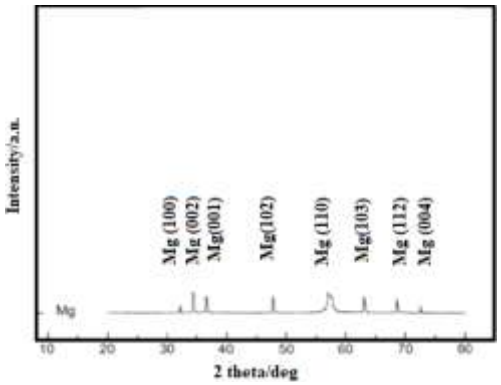

Fig. 2: XRD of Mg-alloy

3.2. Strength and elongation calculations

Tensile strength and percentage elongation is measured according to the procedure provided in section 2.3. The UTM provides the load values and corresponding tensile strength is computed by conventional way as load per unit cross-sectional area. The specimen is prepared according to the testing standard of ASTM E 8M-04. Table 1 gives the values of US, YS and percentage elongation (PE). It has been found that with the decrease in the percentage of additives the US and YS decreases while PE increases.

Table 1: Ultimate & yield strengths and % elongation calculations

Composition	% Additive	US (MPa)	YS (MPa)	(%) Elongation
Mg-6Pa	6	67	51	1.03
Mg-4Pa	4	99	86	1.19
Mg-2Pa	2	108	99	1.57

The main reason behind this is the increase in the porosity of the alloy. With the increase of the additives, the chance of large value of porosity increases during sintering. As the sintering process, evaporates the water and binder, so particles are diffused more closely with each other (as evident from Figs. 3 and 4). This diffusion

of particles increases the US,YS and PE. Figs. 3 and 4 the represents the SEM micrograph of Mg-6Pa and Mg-2Pa. It is evident from the Fig. 3 that additives are fused well and during sintering the voids are increased. The increment in the voids is the result of the temperature increase. Fig. 4 depicts the morphology of Mg-2Pa. Due to less percentage of additive the void size is decreased. All the particles are diffused into one another and porosity final value in Fig. 4 is less.

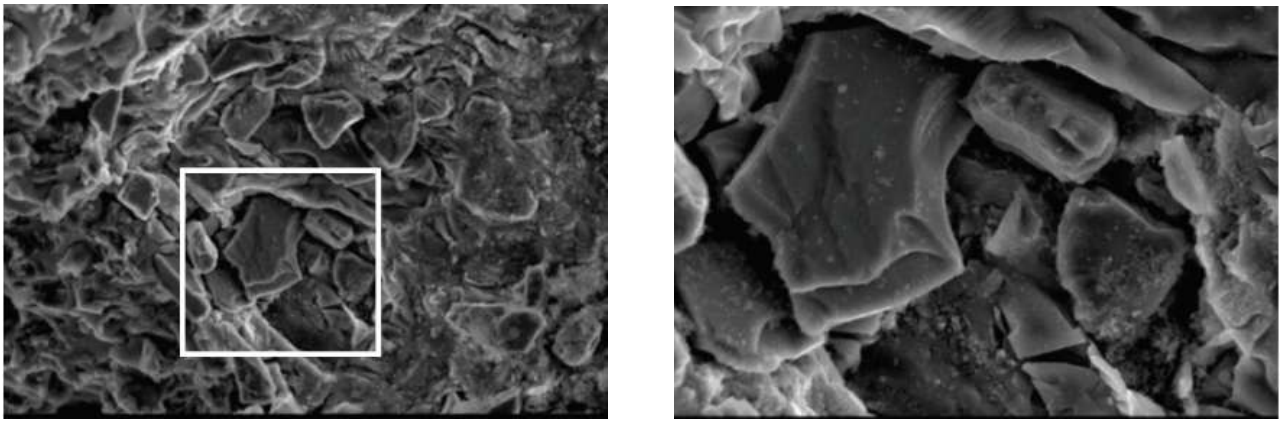

Fig. 3: SEM micrograph of Mg-6Pa (Left); Enlarged view of portion marked (Right)

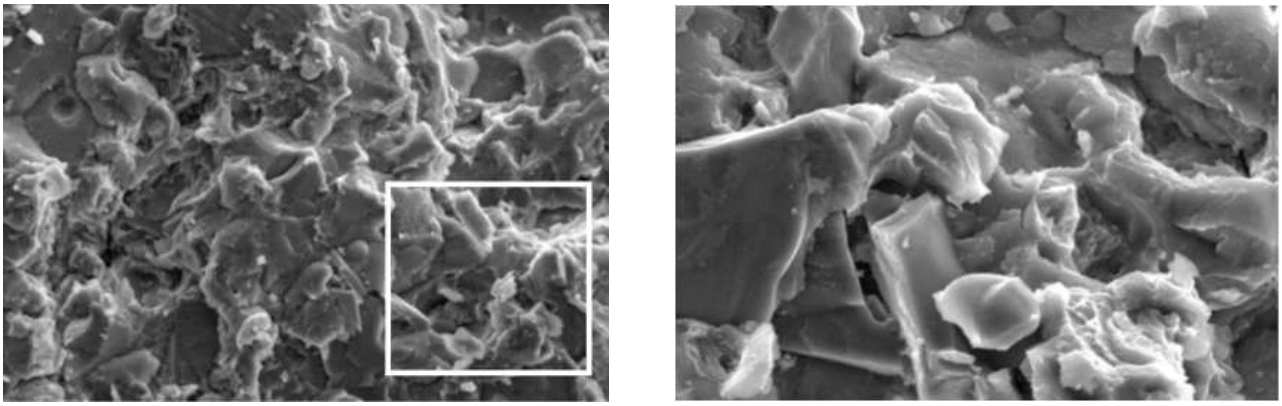

Fig. 4: SEM micrograph of Mg-2Pa (Left); Enlarged view of portion marked (Right)

4. Conclusions

In the present work, Mg-alloys were made by powder metallurgy using organic particles as space holder. The microstructural evaluation of Mg-alloys revealed that the open-cell structure has been formed with uniform pore size and porosity. The pore size of Mg-alloy is 0.42mm. XRD verified the existence of Mg at different orientation of radiation. The mechanical characterization revealed that the tensile strength and PE of alloy increased with decrease in the % additives in the Mg-alloy. The sintering effect on mechanical characteristics can also be evaluated by using other inert atmosphere.

REFERENCES:

[1] B.L. Mordike and T. Ebert. 2001. Magnesium: properties-applications-potential, *Material Sci. and Engg.*; 302, 37-45. https://doi.org/10.1016/S0921-5093(00)01351-4.

[2] H. Somekawa and T. Mukai. 2005. Effect of texture on fracture toughness in extruded AZ31, *Scripta Materialia*, 53(5), 541-545.

[3] X.N. Gu, X.H. Xie, N. Li, Y.F. Zheng and L. Qin. 2012. In vitro and in vivo studies on a Mg-Sr binary alloy system developed as a new kind of biodegradable metal, *Acta Biomat.*, 8, 2360-2374. https://doi.org/10.1016/j.actbio.2012.02.018.

[4] I.S. Berglund, H.S. Brar, N. Dolgova, A.P. Acharya, B.G. Keselowsky, M. Sarntinoranont and M.V. Manuel. 2012. Synthesis and characterization of Mg-Ca-Sr alloys for biodegradable orthopedic implant applications, *J. Biomed. Mat. Res.*, 100, 1524-1534. https://doi.org/10.1002/jbm.b.32721.

[5] X. Zhang, G. Yuan, L. Mao, J. Niu and W. Ding. 2012. Bio-corrosion properties of as-extruded Mg-Nd-Zn-Zr alloy compared with commercial AZ31 and WE43 alloys, *Materials Letters*, 66, 209-211.

[6] X. Gu, Y. Zheng, Y. Cheng, S. Zhong, T. Xi. 2009. In vitro corrosion and biocompatibility of binary magnesium alloys, *Biomaterials*, 30, 484-498. https://doi.org/10.1016/j.biomaterials.2008.10.021.

[7] Y. Huang, W. Gan, K.U. Kainer and N. Hort. 2014. Role of multi-microalloying by rare earth elements in ductilization of magnesium alloys, *J. Magnesium and Alloys*, 2, 1-7. https://doi.org/10.1016/j.jma.2014.01.005.

[8] S. Tekumalla, S. Seetharaman, A. Almajid, M. Gupta 2015. Mechanical properties of magnesium-rare earth alloy systems - A review, *Metals*, 5, 1-39. https://doi.org/10.3390/met5010001.

[9] L.C. Li, J.C. Gao and Y. Wang. 2004. Evaluation of cyto-toxicity and corrosion behaviour of alkali-heat-treated magnesium in simulated body fluid, *Surface Coating Tech.*, 185, 92-98. https://doi.org/10.1016/j.surfcoat.2004.01.004.

[10] G. Song and S. Song. 2010. A possible biodegradable magnesium implant material. *Advanced Engg. Materials*, 9, 298-302. https://doi.org/10.1002/adem.200600252.

[11] L.L. Hench and I. Thompson. 2010. Twenty-first century challenges for biomaterials, *J. Royal Society Interface*, 7, S379-S391. https://doi.org/10.1098/rsif.2010.0151.focus.

[12] http://www.mddionline.com/article/three-generations-biomaterials.

[13] https://www.alliedmarketresearch.com/medical-implants-market.

[14] B. Liu and Y.F. Zheng. 2011. Effects of alloying elements (Mn, Co, Al, W, Sn, B, C and S) on biodegradability and in vitro biocompatibility of pure iron, *Acta Biomat.*, 7, 1407-1420. https://doi.org/10.1016/j.actbio.2010.11.001.

[15] H. Li, Y. Zheng and L. Qin. 2014. Progress of biodegradable metals, progress in natural science, *Materials Int.*, 24, 414-422.

[16] N. Li and Y. Zheng. 2013. Novel magnesium alloys developed for biomedical application - A Review, *J. Material Sci. and Tech.*, 29, 489-502. https://doi.org/10.1016/j.jmst.2013.02.005

[17] D. Ding. 2016. Opportunities and challenges for the biodegradable magnesium alloys as next-generation biomaterials, *Regenerative Biomaterials*, 79-86. https://doi.org/10.1093/rb/rbw003.

[18] N. Sharma, T. Raj and K.K. Jangra. 2016. Microstructural evaluation of Ni Ti-powder, steatite, and steel balls after different milling conditions, *Mat. and Manuf. Proc.*, 31, 628-632. https://doi.org/10.1080/10426914.2015.1004710.

[19] M.N. Samani, A.R. Kamali and R. Mobarra. 2010. Phase transformation of Ni-15 wt. % B powders during mechanical alloying and annealing, *Materials Letters*, 64, 309-312. https://doi.org/10.1016/j.matlet.2009.10.070.

[20] K.K. Mustafa. 2008. Magnesium and its alloys applications in automotive industry, *Int. J. Adv. Manuf. Tech*. 39, 851-865. https://doi.org/10.1007/s00170-007-1279-2.